Assessment of Satellite Chlorophyll-Based Leaf Maximum Carboxylation Rate (Vcmax) Using Flux Observations at Crop and Grass Sites

Xiaojin Qian, Liangyun Liu ⓘ, Xidong Chen ⓘ, and Pablo J. Zarco-Tejada

Abstract—The leaf maximum carboxylation rate (Vcmax) is a key parameter in modeling plant photosynthesis. The rapid and accurate acquisition of Vcmax at large scales can improve understanding of global vegetation productivity and the terrestrial carbon cycle. In this article, we assessed the retrieval of Vcmax from satellite data by validating these data using flux observations made at eight crop and grass sites. Firstly, an empirical model applicable to C_3 species that was based on the semimechanistic linkage between leaf chlorophyll and Vcmax was used to derive Vcmax from satellite data. Then, using vegetation, soil, and meteorological variables as inputs, the SCOPE model was used to estimate Vcmax from half-hourly or hourly flux observations at each site. The estimates of Vcmax were assessed by comparing the simulated gross primary production (GPP) against the observed GPP: that is, the Vcmax value corresponding to its simulated diurnal GPP data with minimum root-mean-square error (RMSE) was selected as the inverted Vcmax value. Finally, the Vcmax values retrieved from MERIS and Sentinel-3 OLCI satellite data were validated using the *in situ* flux site observations. The results showed that the estimates of Vcmax based on satellite data successfully captured the seasonal variations in Vcmax retrieved from the tower-based GPP data, giving a mean RMSE value of 15.30 μmol m^{-2} s^{-1}. Our results support the retrieval of Vcmax from satellite data based on the link with leaf chlorophyll content and show that there was good agreement between Vcmax derived from remote sensing and flux data.

Index Terms—Gross primary production (GPP), leaf chlorophyll content (Cab), leaf maximum carboxylation rate (Vcmax), MERIS, SCOPE, Sentinel-3 OLCI.

I. INTRODUCTION

PLANT photosynthesis, a process that converts carbon dioxide into sugars, provides most of the energy needed for life [1]–[3]. As this process is a crucial part of the ecosystem carbon cycle, accurate modeling of photosynthesis is particularly necessary [4].

Currently, the Farquhar–von Caemmerer–Berry leaf biochemical model [5] embedded in most terrestrial biosphere models is widely used to simulate photosynthesis. This model involves two critical parameters: the leaf maximum carboxylation rate (Vcmax) and the maximum electron transport rate (Jmax) normalized to a reference temperature of 25°C. Vcmax controls CO_2 fixation within the carbon reaction process. Therefore, it is essential to accurately derive Vcmax because of its decisive significance in photosynthesis models.

Traditionally, Vcmax is measured using gas-exchange measurements, which is time-consuming and laborious. The lack of temporally and spatially continuous Vcmax data precludes the estimation of gross primary production (GPP) accurately at the global scale. Time-series data can be obtained quickly and at a large scale using remote sensing, thus possibly solving the problems mentioned above. In contrast to leaf pigment content, the photosynthetic parameter Vcmax has no obvious spectral response mechanisms, but is closely related to the leaf characteristics [6]–[8]. It has been shown that the nitrogen content corresponding to the Rubisco enzyme shows a strong correlation with Vcmax [9]. Nevertheless, it is difficult to accurately retrieve the nitrogen content from remote sensing data as the relevant spectral response bands are easily influenced by the foliar water content, cellular structure scattering and atmospheric water vapor [10], [11]. Chlorophyll, at the light-harvesting apparatus, plays a crucial role in photosynthesis [12]. In recent years, many researchers have theoretically and experimentally demonstrated a good correlation between Vcmax and the leaf chlorophyll content (Cab) [13]–[16]. The usefulness of Cab as a proxy for Vcmax at large scales depends on the ability to accurately retrieve chlorophyll from satellite data [17]. Compared with nitrogen, the spectral response mechanism for chlorophyll is much clearer. The spectral bands sensitive to chlorophyll are mainly located in the visible and red-edge spectral regions, which are much less disturbed by external factors. Moreover, some multispectral and hyperspectral sensors can acquire spectral data in the red-edge region, which allows the leaf Cab to be accurately estimated. Therefore, remotely sensed can be used as a good proxy for leaf Vcmax at large spatial scales.

Xiaojin Qian and Xidong Chen are with the Aerospace Information Research Institute, Chinese Academy of Sciences, Beijing 100094, China, and also with the University of Chinese Academy of Sciences, Beijing 100049, China (e-mail: qianxj@radi.ac.cn; chenxd@radi.ac.cn).

Liangyun Liu is with the Aerospace Information Research Institute, Chinese Academy of Sciences, Beijing 100094, China (e-mail: liuly@radi.ac.cn).

Pablo J. Zarco-Tejada is with the School of Agriculture and Food, Faculty of Veterinary and Agricultural Sciences, and Department of Infrastructure Engineering, Faculty of Engineering and Information Technology, University of Melbourne, Melbourne, VIC 3010, Australia, and also with the Instituto de Agricultura Sostenible, Consejo Superior de Investigaciones Científicas, 14004 Cordoba, Spain (e-mail: pablo.zarco@unimelb.edu.au).

TABLE I
INFORMATION ABOUT THE SITES USED IN THIS ARTICLE

Site ID	Latitude	Longitude	Study period	Source	IGBP land cover classification	Reference
DE-Geb	51.1001	10.9143	2003−2010	Fluxnet2015	Cropland	Anthoni, *et al.* [28]
DE-Gri	50.9495	13.5125	2004−2011	Fluxnet2015	Grassland	Prescher, *et al.* [29]
DE-Kli	50.8929	13.5225	2004−2011	Fluxnet2015	Cropland	
US-Ne2	41.1649	-96.4701	2004, 2006, 2008	Fluxnet2015	Cropland	Verma, *et al.* [30]
US-Ne3	41.1797	-96.4397	2004, 2006, 2008, 2010	Fluxnet2015	Cropland	
US-Bi1	38.0992	-121.4993	2019	Ameriflux	Cropland	Hemes, *et al.* [31]
US-Sne	38.0369	-121.7547	2019	Ameriflux	Grassland	
US-Snf	38.0400	-120.7272	2019	Ameriflux	Grassland	Li, *et al.* [32]

So far, only a small number of studies have been conducted with the aim of retrieving Vcmax from satellite data. To meet the needs of photosynthesis and vegetation productivity simulation studies, it is essential to make progress on the retrieval, interpretation and validation of Vcmax derived from airborne and satellite multispectral and hyperspectral sensors. Thus, it is necessary to develop methods for accurately estimating Vcmax that can overcome the validation constraints caused by insufficient ground truth data and spatial scale mismatches [8]. The GPP usually represents the sum of the photosynthesis rates of all leaves at the ecosystem scale [18]. It has been shown that eddy covariance (EC) flux measurements can offer an effective approach for deriving Vcmax from CO_2 fluxes [4], [19], [20]. In some studies, Vcmax has been successfully retrieved from sun-induced fluorescence (SIF) [20]–[23] derived from airborne hyperspectral data [24] using the SCOPE model [20], [21], [23], [25]. However, except for airborne imagers, the spatial resolution of SIF products is usually very coarse [26]. Even though the OCO-2 SIF product has a relatively high spatial resolution (1.29×2.25 km), its actual applicability to making estimates of Vcmax is more limited than for chlorophyll products retrieved from other satellite sensors, such as Sentinel-3 OLCI [18].

In terms of modeling, Vcmax is a key leaf biochemical parameter used in the SCOPE model, which is used to simulate photosynthesis [27]. As a result, the retrieval of Vcmax from flux observations through inversion of the SCOPE model provides an indirect, operational approach to validating Vcmax values derived from satellite data. In this article, we retrieved leaf Vcmax from satellite data and validated it using Vcmax data that were derived from CO_2 tower fluxes by SCOPE model inversion. An empirical model based on a semimechanistic method linking leaf chlorophyll and Vcmax was used to estimate leaf Vcmax from satellite data. This assessment of Vcmax will be help to understanding the performance of SCOPE model inversion as used in an operational approach with satellite data and thus contribute to an understanding of the uncertainty in model simulations of photosynthesis and vegetation productivity.

II. MATERIALS AND METHODS

A. Flux Tower Sites

Eight cropland and grassland sites from the Fluxnet2015 and Ameriflux datasets were selected for use in the validation. The selection of the study period was mainly based on the availability of flux tower meteorological data, CO_2 flux data, satellite data, and the homogeneity of the underlying surfaces at these sites. At both the US-Ne2 and US-Ne3 sites, corn and soybean are grown in alternate years (corn in "odd" years and soybean in "even" years). Since this article was focused on C_3 plants, only even-year data were selected for these two sites. Details of the flux tower sites used in this article are given in Table I.

B. Flux, Meteorological, and Satellite Data

Flux and associated meteorological data for the eight sites were acquired from the Fluxnet2015 website[1] and the AmeriFlux website.[2] For the AmeriFlux data, gap filling, and flux partitioning were carried out using the REddyProc package in [33] produced by the Max Planck Institute for biogeochemistry. The Fluxnet2015 Dataset integrates the flux measurements from multiple regional flux networks and provides GPP estimates and corresponding meteorological data. Half-hourly and hourly meteorological data were used to run the SCOPE model. Gap-filled longwave radiation, shortwave radiation, air temperature, vapor pressure deficit, atmospheric pressure, wind speed, and the CO_2 mole fraction were reprocessed for use as the forcing variables in SCOPE to produce continuous half-hourly and hourly GPP estimates. The GPP flux data used for the above sites were derived from EC flux measurements. They were estimated as the difference between the ecosystem respiration and net ecosystem exchange at half-hourly or hourly intervals using a night-time flux-partitioning algorithm [34].

In order to test the approaches described in this study using a long data series, MERIS data from 2003 to 2011 were used to retrieve the Cab and leaf area index (LAI). This dataset was chosen because it has red-edge and near-infrared bands, a high spectral resolution, medium spatial resolution (300 m) and a short revisit cycle (2–3 days) [35]. The seven-day full resolution surface reflectance product produced by the synthesis of images was used [36]. MERIS is no longer in operation—it was in operation from 2003 to 2012. For the flux tower sites described above, the band 7 (665 nm), band 8 (681.25 nm), band 9 (708.75 nm) and band 12 (778.75 nm) surface reflectances were extracted for use as inputs to the Cab and LAI inversion algorithms. This will be described in the following section.

---

[1][Online]. Available: http://fluxnet.fluxdata.org/data/fluxnet2015-dataset/
[2][Online]. Available: https://ameriflux.lbl.gov/

Sentinel-3 OLCI, the successor to MERIS, has band settings that are highly similar to those of MERIS. The level-2 SYN product (SY_2_SYN) is produced by the synergy level-2 processor and contains surface reflectance and aerosol parameters for land areas. Since the level-2 SYN product is currently available only for September 2018 onward, data from 2019 were selected for assessment. The band 8 (665 nm), band 10 (681.25 nm), band 11 (708.75 nm) and band 16 (778.75 nm) surface reflectances were extracted from the seven-day level-2 SYN product for the retrieval of Cab and LAI.

C. Inversion of Cab and LAI

Leaf Cab was estimated from the MERIS and OLCI surface reflectances according to the algorithm described in Qian and Liu [37] using an improved look-up-table (LUT) approach that combined multiple canopy structures and soil backgrounds. Canopy spectra were simulated using the PROSAIL-D model with a range of leaf biochemical parameters, canopy structures, soil reflectance values and imaging geometries as the inputs. The LUT consisted of 25 sub-LUTs, corresponding to five different types of canopy structure and five types of soil background. For each sub-LUT, the mean of the eight best solutions corresponding to the eight smallest root-mean-square error (RMSE) values was selected as the inverted Cab value. The average of the 25 sub-LUT inversion results was then taken as the final inversion result. Validation of the inversion results using field-measured canopy spectra and MERIS imagery yielded RMSE values lower than 10 μg cm^{-2}.

Many studies have shown that the normalized difference vegetation index (NDVI) suffers from saturation at moderate to high LAI values, which limits its application in LAI retrieval [38], [39]. In order to deal with this issue, Gitelson [38] proposed the wide dynamic range vegetation index (WDRVI) by introducing a weighting coefficient, and claimed that its sensitivity to the moderate-to-high LAI values was three times better than that of the NDVI. In its original form, the WDRVI could be negative for low to moderate vegetation density. Therefore, Peng and Gitelson [40] made some adjustments to the original formula in order to avoid this phenomenon. Subsequently, Nguy-Robertson et al. [39] further improved the form of WDRVI for MERIS spectral bands and constructed a functional relationship between LAI and WDRVI for four crop types. Validation of the LAI results gave R^2 values greater than 0.9. In the article, the following formulas were used to estimate the LAI:

$$\text{WDRVI} = \frac{\alpha \times R_{\text{nir}} - R_{\text{red-edge}}}{\alpha \times R_{\text{nir}} + R_{\text{red-edge}}} + \frac{1 - \alpha}{1 + \alpha}, \ \alpha = 0.1 \quad (1)$$

and

$$\text{LAI} = -1.6 \times \text{WDRVI}^2 + 9.6 \times \text{WDRVI} - 0.29 \quad (2)$$

where R_{nir} and $R_{\text{red-edge}}$ are the near-infrared and red-edge reflectance, respectively, and α is the weighting coefficient.

D. Estimation of Vcmax Derived From Satellite Data

The leaf Vcmax was estimated using satellite remote sensing data based on a semimechanistic approach that coupled leaf Vcmax with Cab (as summarized by Houborg et al. [17].)
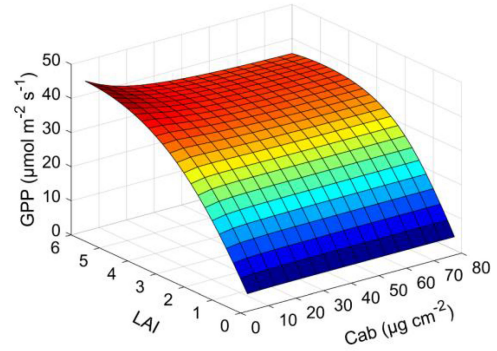

Fig. 1. GPP values simulated by the SCOPE model as a function of Cab (5–80 μg cm^{-2}, intervals of 5 μg cm^{-2}) and LAI (0.25–6, intervals of 0.25).

According to Friend [41], Vcmax can be described as a function of the leaf nitrogen content (N), fraction of leaf nitrogen in Rubisco and catalytic (Rubisco) turnover rate at 25°C (Kcat$_{25}$). Houborg et al. [17] gave the linear regression relationships between Rubisco and N and between N and Cab for C$_3$ plant species. Vcmax was, thus, calculated from Cab using

$$\text{Vcmax} = 2.5294 \times \text{Cab} \left(\mu\text{g cm}^{-2} \right) - 27.34 \left(\mu\text{mol m}^{-2}\text{s}^{-1} \right). \quad (3)$$

E. SCOPE Model

The SCOPE model can be used to simulate the net photosynthesis of canopy (NPC), which is the gross primary productivity minus the dark respiration of the leaf [42]. In this article, GPP was computed from NPC by setting the respiration parameter to zero so that the calculated values could be compared with the GPP observations obtained from the EC flux measurements.

Performing GPP simulations in the SCOPE model requires meteorological parameters (air temperature and pressure, atmospheric vapor pressure, wind speed, CO$_2$ concentration, and incoming shortwave and longwave radiation), and four other kinds of parameters: leaf optical properties, including Cab, dry matter content (Cdm), leaf equivalent water thickness (Cw), and leaf mesophyll structure (N); leaf biochemistry parameters, including the leaf maximum carboxylation capacity at 25°C (Vcmax), stomatal conductance (m) and a respiration parameter (Rdparam); canopy structure parameters, including the LAI and leaf angle distribution (LIDFa and LIDFb); and observation geometry parameters, including the solar zenith angle (tts) and observation zenith angle (tto). These input parameters were obtained from three sources: model inversion; the flux dataset; and relevant literature. Table II gives the main input parameters used in SCOPE in this article.

An example of GPP simulations for different values of Cab (5–80 μg cm^{-2}, intervals of 5 μg cm^{-2}) and LAI (0.25–6, intervals of 0.25) is shown in Fig. 1. It can be seen from Fig. 1 that changes in Cab have only a small effect on the simulated values of GPP. However, the GPP is significantly affected by LAI, with a higher LAI leading to a greater GPP value. In this study, in order to avoid logical errors, the value of Cab inverted from remote sensing data used in the SCOPE model was set to the mean value of each site for the year. The leaf angle distribution

TABLE II
VALUES OR SOURCES OF THE MAIN INPUT PARAMETERS OF THE SCOPE MODEL USED IN THIS ARTICLE

| Parameter	Definition	Unit	Value/source
Leaf optical			
Cab	Chlorophyll a+b content	$\mu g\ cm^{-2}$	Inversion
Cdm	Dry matter content	$g\ cm^{-2}$	0.004
Cw	Leaf equivalent water thickness	cm	0.02
N	Leaf mesophyll structure parameter	—	1.5
Leaf biochemistry			
Vcmax	Maximum carboxylation capacity at 25°C	$\mu mol\ m^{-2}\ s^{-1}$	5–200, step 5
m	Ball-Berry stomatal conductance parameter	—	9
Rdparam	Parameter for dark respiration (Respiration=Rdparam $*\ V_{cmax}$)	—	0
Canopy			
LAI	Leaf area index	$m^2\ m^{-2}$	Inversion
LIDFa	Leaf inclination distribution of leaves	—	−0.35
LIDFb	Variation in leaf inclination	—	−0.15
Meteorology			
Rin	Broadband incoming shortwave radiation (0.4–2.5 μm)	$W\ m^{-2}$	Measurement
Ta	Air temperature	T	Measurement
Rli	Broadband incoming longwave radiation (2.5–50 μm)	$W\ m^{-2}$	Measurement
p	Air pressure	hPa	Measurement
ea	Atmospheric vapor pressure	hPa	Measurement
u	Wind speed at measurement height	$m\ s^{-1}$	Measurement
Ca	Atmospheric CO_2 concentration	ppm	Measurement
Geometry			
LAT	Latitude	deg	Measurement
LON	Longitude	deg	Measurement
tts	Solar zenith angle	deg	30
tto	Observation zenith angle	deg	0
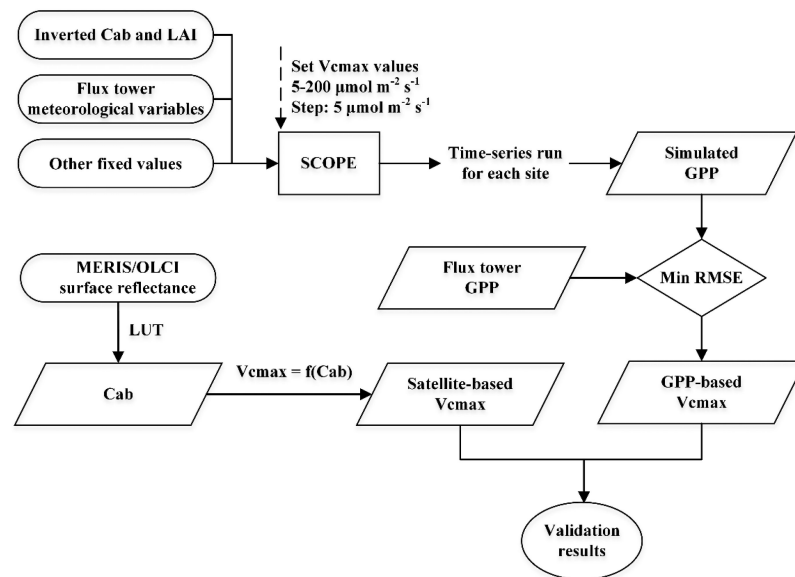
Fig. 2.   Schematic diagram of the process used for validating the satellite-based Vcmax value.

was assumed to be spherical [20], [43], [44]. Subsequently, the Vcmax values were used to build the Vcmax-GPP lookup table.

F. Framework Used to Validate Vcmax Values Derived From Satellite Data

A schematic diagram of the process used to validate the satellite-based Vcmax values is shown in Fig. 2. First, using the vegetation, soil and meteorological parameters as inputs,

SCOPE was run with an LUT containing different Vcmax values corresponding to half-hourly or hourly time intervals for each site. Based on the literature [45], [46], the range of Vcmax was set to 5–200 μmol m^{-2} s^{-1}, divided into 40 intervals of 5 μmol m^{-2} s^{-1}. Thus, for each site, a time series consisting of half-hourly or hourly GPP values under 40 sets of Vcmax conditions could be obtained. By comparing the simulated GPP values against the observed values, the optimal daily Vcmax was retrieved using the minimum RMSE method. For the *j*th
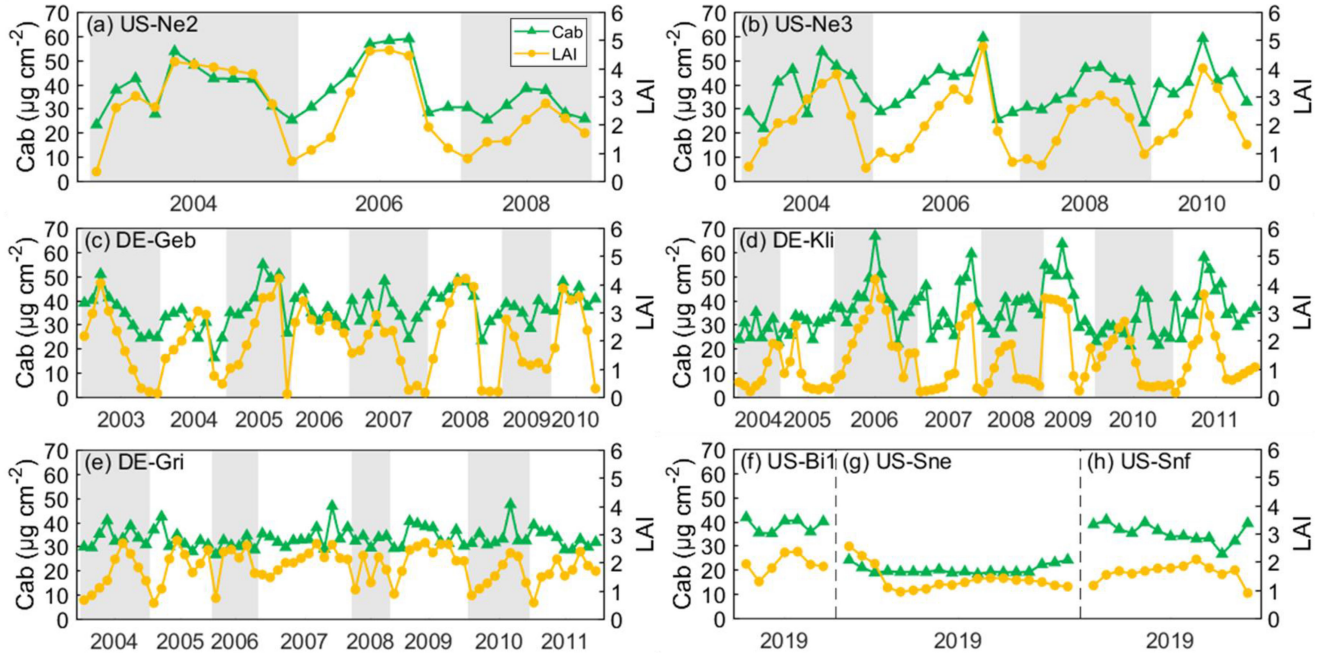
Fig. 3.   Temporal variations in Cab (green) and LAI (yellow) at (a) US-Ne2. (b) US-Ne3. (c) DE-Geb. (d) DE-Kli. (e) DE-Gri. (f) US-Bi1. (g) US-Sne. (h) US-Snf.

Vcmax value, the RMSE between the simulated half-hourly or hourly GPP value GPP_{sim}, and the measured value GPP_{mea}, was calculated as

$$\mathrm{RMSE}\ (j) = \frac{\sum_{m=1}^{M} \left(GPP_{sim}\left(j, m\right) - GPP_{mea}\left(m\right)\right)^2}{M} \tag{4}$$

where m is the mth GPP measurement and M is the total number of measurements (including only daytime GPP measurements). The value of Vcmax that produced the lowest RMSE was selected as the retrieved Vcmax value for the day. Finally, the inverted GPP-based Vcmax value was compared with the chlorophyll-based value of Vcmax to validate the accuracy of retrieving Vcmax using remote sensing satellite data.

III. Results

A. Retrieval Results for Cab and LAI

The leaf Cab estimated by LUT inversion and by using the vegetation index WDRVI are shown in Figs. 3 and 4. The Cab of crops varies from 15 to 70 μg cm^{-2} with one or more peaks in the growing season; for grasses, the Cab values exhibit less seasonal variability, varying between 15 and 50 μg cm^{-2}. In general, the Cab values of the crops are higher than those of the grasses, with the average value for the crops being in the range of 30–40 μg cm^{-2}. Consistent with the distribution of Cab values, the range of LAI values for crops is also larger than that for grasses. It can also be seen that, during the course of a growing season, the LAI values change more than the Cab values: compared with the clear seasonal patterns in the LAI, the Cab is relatively stable. The same crops were grown at the US-Ne2 and US-Ne3 sites, but using different irrigation schemes. The difference in crop growth conditions caused by differences in irrigation is clearly reflected in the distribution of the estimated LAI values. These
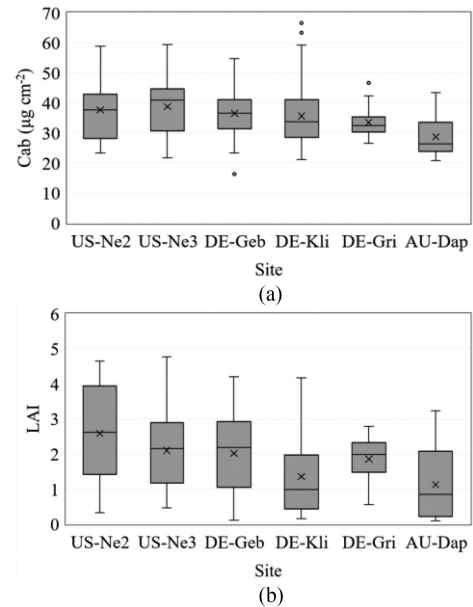

Fig. 4.   Distributions of (a) Cab and (b) LAI values for the eight sites. In each box, the cross and horizontal line represent the mean and median, respectively; the bottom and top of each box are the 25th and 75th quartiles, respectively. The lower whisker extends to the minimum value and the upper whisker to the maximum value. The gray dot is an outlier datum point.

results indicate that the inverted Cab and LAI values were within the expected ranges throughout the growing season.

B. Variations of Inverted and Estimated Vcmax

The temporal variation in the Vcmax values derived from satellite data (denoted by Vcmax_Cab) was also evaluated. The Vcmax_Cab values exhibit good agreement with the values
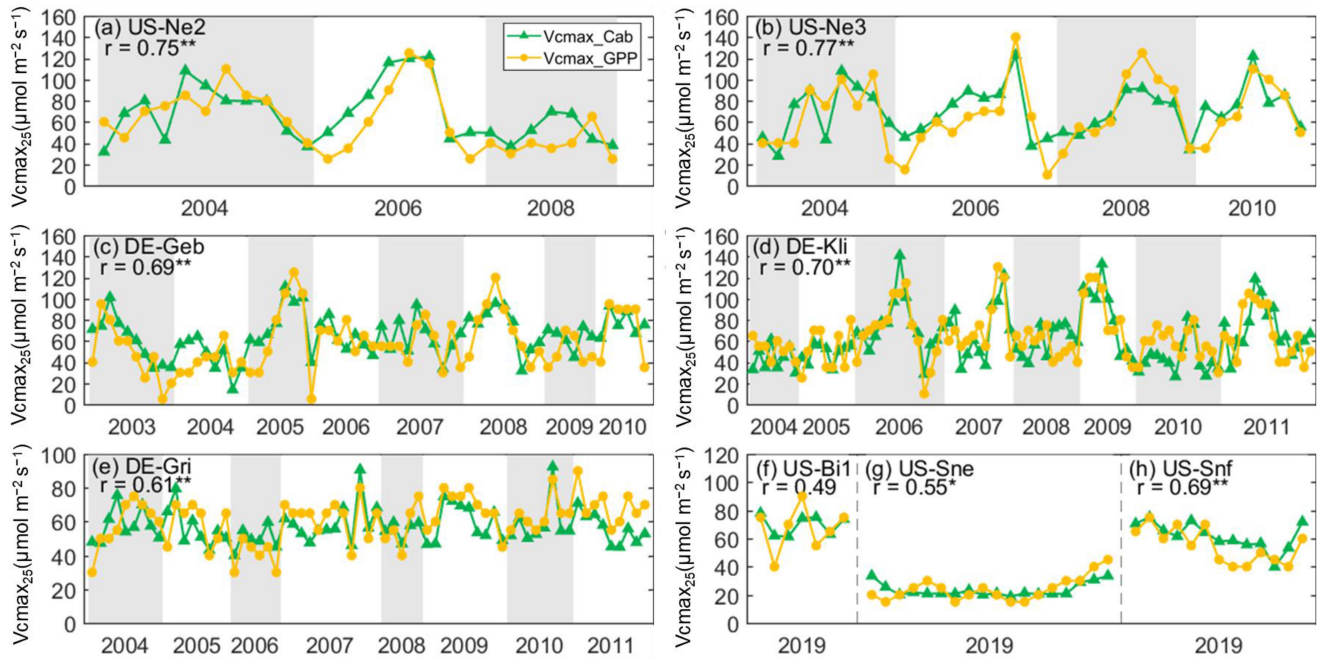
Fig. 5. Temporal variations in Vcmax_Cab (green) and Vcmax_GPP (yellow) at (a) US-Ne2. (b) US-Ne3. (c) DE-Geb. (d) DE-Kli. (e) DE-Gri. (f) US-Bi1. (g) US-Sne. (h) US-Snf. The single and double asterisks represent significant correlation at the 0.05 and 0.01 levels, respectively.
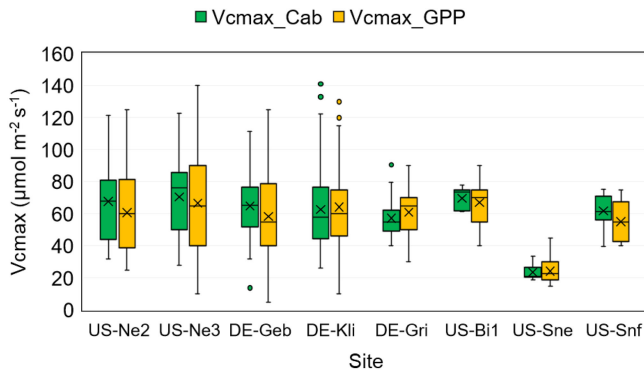

Fig. 6. Distributions of Vcmax_Cab and Vcmax_GPP values for the eight sites.

of Vcmax estimated from flux observations (denoted by Vcmax_GPP) (see Fig. 5). Although Vcmax_Cab missed certain variations, it successfully captured the overall trends. Except for US-Bi1 and US-Sne, significant linear correlation was found between Vcmax_Cab and Vcmax_GPP at the other six sites. The Vcmax_Cab values at the US-Ne3 site performed best in terms of tracking the seasonal variation in Vcmax. However, at US-Sne, the estimates were unsatisfactory: this may have been a result of the continuously very low LAI leading to errors in the inversion of Cab. Moreover, the histograms also suggest that the distribution of Vcmax_Cab is similar to that obtained for Vcmax_GPP (see Fig. 6). Although the values of Vcmax_Cab do not accurately characterize the photosynthetic capacity at the beginning, end and peak of the growth period, the Vcmax values derived from satellite data are reasonable.

C. Validation of Satellite-Based Vcmax

Fig. 7 shows comparisons between Vcmax_Cab and Vcmax_GPP. This validation indicates that, for the crops and grasses used in this study, about 44% of the variance in Vcmax_Cab can be explained by linear regression models. The smallest RMSE (6.864 μmol m^{-2} s^{-1}) is for the US-Sne site and the largest (20.771 μmol m^{-2} s^{-1}) is for US-Ne2. The Vcmax values estimated from satellite data show either a slight overestimation or underestimation, depending on the site, with biases of 7.042, 3.924, 6.605, −1.630, −3.586, 2.520, 1.910, and 4.005 μmol m^{-2} s^{-1} for US-Ne2, US-Ne3, DE-Geb, DE-Kli, DE-Gri, US-Bi1, US-Sne, and US-Snf, respectively.

IV. DISCUSSION

The article presented here demonstrates that the values of leaf Vcmax derived from satellite chlorophyll retrievals followed the trends observed in the Vcmax values estimated from CO_2 flux towers by inverting the SCOPE model. However, Cab–Vcmax and GPP–Vcmax relationships are influenced by leaf and canopy properties, spatial and temporal scales, and other confounding factors [47], and these influences need to be accounted for using proper radiative transfer modeling methods. The limitations of and uncertainties in the methods used in this article are a result of factors related to both the data used and the models themselves. The model inputs introduce errors as a result of the parameters required to carry out the SCOPE model inversions. The limitations of the SCOPE model itself and the simplifications introduced as part of the validation process are also sources of uncertainty.

The uncertainties in Cab and LAI retrieved by satellite data propagate through to the simulations of the GPP. To avoid logical
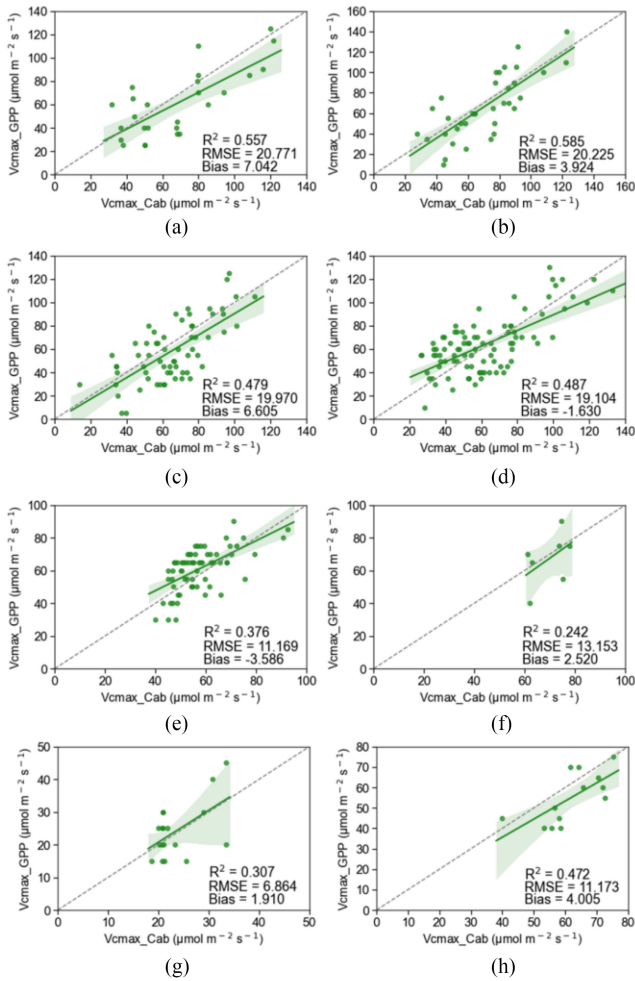
Fig. 7. Relationship between Vcmax_Cab and Vcmax_GPP at (a) US-Ne2. (b) US-Ne3. (c) DE-Geb. (d) DE-Kli. (e) DE-Gri. (f) US-Bi1. (g) US-Sne. (h) US-Snf. The green shaded area represents the 95% confidence interval. The dotted grey line is the 1:1 line.

loop errors, the Cab was set to the mean value of each site for the year because of the small effect this had on the simulation of GPP in SCOPE. Also, in other studies, leaf chlorophyll parameters have not been used as input parameters for simulating GPP [4], [19], [23]. However, accurate Cab inversion might improve the accuracy of GPP simulation to a certain extent, especially at the start and end of the growth periods. The LAI is one of the key parameters in GPP simulation [48]–[51]. In this article, vegetation index-based LAI was selected for use. However, the applicability of the LAI–VI relationship is limited by many external factors, including the vegetation type, observation geometry, and background reflectance [52]. Moreover, when using the SCOPE model to simulate the GPP, several parameters were set as fixed values, which will have produced additional uncertainties in the inversion results: for example, in many previous studies, the canopy structure was assumed to be spherical for crops and grasses. Such an assumption is reasonable under specific conditions, but needs to be carefully considered when it is applied at large scales. Since this article focused on the growing season, it was assumed that the effect of the uncertainty in the LAI and Cab was generally small. It

should be noted that because SCOPE is a 1-D model that assumes homogeneity in the horizontal direction, the model may not be applicable to heterogeneous conditions [27]. The layer concept used in the model limits assessment of the effects of multiple scattering [53]. Thus, this article focused only on validation of Vcmax for two types of vegetation—crops and grass. In addition, the difference between the size of the flux footprint and the size of the satellite pixels and between daily Vcmax_GPP and seven-day synthesized Vcmax_Cab are additional sources of uncertainty.

Since the leaf Cab is the core link used for the inversion of Vcmax, the retrieval of the Cab is an important precondition for the application of the method used in this article. The chlorophyll inversion method used in this article is only applicable to vegetation types for which the clumping effect can be neglected. Therefore, it is still necessary to develop a chlorophyll inversion algorithm suitable for vegetation with complex canopy structures. Even for C_3 vegetation types, different studies have established different Cab–Vcmax relationships, for which there are many influencing factors, such as vegetation types, leaf-water stress status, leaf age, etc. [12], [13], [17]. Therefore, a comprehensive comparative analysis and selection of appropriate functional relationships can help with obtaining accurate values of leaf Vcmax. The validation results presented in this study aid progress on the use of leaf Cab as a proxy for leaf Vcmax and have strong potential for use in explicit mapping of Vcmax at large spatial scales. As this article concerned crops and grasses only, validation of this approach for other ecosystems is still required.

V. Conclusion

Vcmax is a critical physiological parameter used in the modeling of photosynthesis at large scales and requires frequent quantification. Although several studies have proved that leaf Vcmax can be retrieved from spectra based on the relationship with leaf Cab, the retrieval of Vcmax from satellite data has been carried out in only a few of these. In this article, we retrieved leaf Vcmax from satellite data and validated it using Vcmax values obtained from CO_2 flux towers by inverting the SCOPE model. The results indicated that Vcmax estimated from satellite Cab retrievals successfully captured the seasonal variations in Vcmax estimated from the flux tower data, giving a mean R^2 value of 0.44 and a mean RMSE value of 15.30 μmol m^{-2} s^{-1} for eight different validation sites. The results of this article illustrate that leaf Vcmax derived from satellite data based on the link with leaf Cab can be used for the operational monitoring of photosynthesis at a global scale.

References

[1] D. A. Bryant, and N.-U. Frigaard, "Prokaryotic photosynthesis and phototrophy illuminated," *Trends Microbiol.,* vol. 14, no. 11, pp. 488–496, 2006.

[2] C. Beer *et al.*, "Terrestrial gross carbon dioxide uptake: Global distribution and covariation with climate," *Science,* vol. 329, no. 5993, pp. 834–838, 2010.

[3] A. Gonsamo, J. M. Chen, and D. Lombardozzi, "Global vegetation productivity response to climatic oscillations during the satellite era," *Global Change Biol,* vol. 22, no. 10, pp. 3414–3426, 2016.

[4] X. Xie, A. Li, H. Jin, G. Yin, and X. Nan, "Derivation of temporally continuous leaf maximum carboxylation rate (Vcmax) from the sunlit leaf gross photosynthesis productivity through combining BEPS model with light response curve at tower flux sites," *Agricultural Forest Meteorol.,* vol. 259, pp. 82–94, 2018.

[5] G. D. Farquhar, S. von Caemmerer, and J. A. Berry, "A biochemical model of photosynthetic CO_2 assimilation in leaves of C3 species," *Planta,* vol. 149, no. 1, pp. 78–90, 1980.

[6] S. P. Serbin, D. N. Dillaway, E. L. Kruger, and P. A. Townsend, "Leaf optical properties reflect variation in photosynthetic metabolism and its sensitivity to temperature," *J. Exp. Botany,* vol. 63, no. 1, pp. 489–502, 2012.

[7] C. R. Yendrek *et al.*, "High-throughput phenotyping of maize leaf physiological and biochemical traits using hyperspectral reflectance," *Plant Physiol.,* vol. 173, no. 1, pp. 614–626, 2017.

[8] P. Fu, K. Meacham-Hensold, K. Guan, J. Wu, and C. Bernacchi, "Estimating photosynthetic traits from reflectance spectra: A synthesis of spectral indices, numerical inversion, and partial least square regression," *Plant Cell Environ.,* vol. 42, no. 5, pp. 1242–1258, 2020.

[9] Ü. Niinemets and J. D. Tenhunen, "A model separating leaf structural and physiological effects on carbon gain along light gradients for the shade-tolerant species *Acer saccharum*," *Plant Cell Environ.,* vol. 20, no. 7, pp. 845–866, 1997.

[10] I. Herrmann, A. Karnieli, D. J. Bonfil, Y. Cohen, and V. Alchanatis, "SWIR-based spectral indices for assessing nitrogen content in potato fields," *Int. J. Remote Sens.,* vol. 31, no. 19, pp. 5127–5143, 2010.

[11] Y. Knyazikhin *et al.*, "Hyperspectral remote sensing of foliar nitrogen content," *Proc. Nat. Acad. Sci.,* vol. 110, no. 3, pp. E185-E192, 2013.

[12] S. Wang *et al.*, "Estimation of leaf photosynthetic capacity from leaf chlorophyll content and leaf age in a subtropical evergreen coniferous plantation," *J. Geophys. Res., Biogeosci.,* vol. 125, no. 2, 2020, Art. no. e2019JG005020.

[13] H. Croft, J. M. Chen, X. Luo, P. Bartlett, B. Chen, and R. M. Staebler, "Leaf chlorophyll content as a proxy for leaf photosynthetic capacity," *Global Change Biol.,* vol. 23, no. 9, pp. 3513–3524, Aug. 2017.

[14] X. Qian, Y. Zhang, L. Liu, and S. Du, "Exploring the potential of leaf reflectance spectra for retrieving the leaf maximum carboxylation rate," *Int. J. Remote Sens.,* vol. 40, no. 14, pp. 5411–5428, Feb. 2019.

[15] X. Luo, H. Croft, J. M. Chen, P. Bartlett, R. Staebler, and N. Froelich, "Incorporating leaf chlorophyll content into a two-leaf terrestrial biosphere model for estimating carbon and water fluxes at a forest site," *Agricultural Forest Meteorol.,* vol. 248, pp. 156–168, 2018.

[16] P. B. Alton, "Retrieval of seasonal Rubisco-limited photosynthetic capacity at global FLUXNET sites from hyperspectral satellite remote sensing: Impact on carbon modelling," *Agricultural Forest Meteorol.,* vol. 232, pp. 74–88, 2017.

[17] R. Houborg, A. Cescatti, M. Migliavacca, and W. P. Kustas, "Satellite retrievals of leaf chlorophyll and photosynthetic capacity for improved modeling of GPP," *Agricultural Forest Meteorol.,* vol. 177, pp. 10–23, 2013.

[18] S. Chou *et al.*, "Estimation of leaf photosynthetic capacity from the photochemical reflectance index and leaf pigments," *Ecol. Indicators,* vol. 110, 2020, Art. no. 105867.

[19] T. Zheng *et al.*, "Inverting the maximum carboxylation rate (Vcmax) from the sunlit leaf photosynthesis rate derived from measured light response curves at tower flux sites," *Agricultural Forest Meteorol.,* vol. 236, pp. 48–66, 2017.

[20] Y. Zhang, L. Guanter, J. Joiner, L. Song, and K. Guan, "Spatially-explicit monitoring of crop photosynthetic capacity through the use of space-based chlorophyll fluorescence data," *Remote Sens. Environ.,* vol. 210, pp. 362–374, 2018.

[21] Y. Zhang *et al.*, "Estimation of vegetation photosynthetic capacity from space-based measurements of chlorophyll fluorescence for terrestrial biosphere models," *Global Change Biol.,* vol. 20, no. 12, pp. 3727–3742, Dec. 2014.

[22] K. Guan *et al.*, "Improving the monitoring of crop productivity using spaceborne solar-induced fluorescence," *Global Change Biol.,* vol. 22, no. 2, pp. 716–726, 2016.

[23] L. He *et al.*, "Diverse photosynthetic capacity of global ecosystems mapped by satellite chlorophyll fluorescence measurements," *Remote Sens. Environ.,* vol. 232, 2019, Art. no. 111344.

[24] C. Camino, V. Gonzalez-Dugo, P. Hernandez, and P. J. Zarco-Tejada, "Radiative transfer vcmax estimation from hyperspectral imagery and SIF retrievals to assess photosynthetic performance in rainfed and irrigated plant phenotyping trials," *Remote Sens. Environ.,* vol. 231, 2019, Art. no. 111186.

[25] E. N. Koffi, P. J. Rayner, A. J. Norton, C. Frankenberg, and M. Scholze, "Investigating the usefulness of satellite derived fluorescence data in inferring gross primary productivity within the carbon cycle data assimilation system," *Biogeosciences,* vol. 12, no. 1, pp. 4067–4084, 2015.

[26] G. H. Mohammed *et al.*, "Remote sensing of solar-induced chlorophyll fluorescence (SIF) in vegetation: 50 years of progress," *Remote Sens. Environ.,* vol. 231, 2019, Art. no. 111177.

[27] C. Van der Tol, W. Verhoef, J. Timmermans, A. Verhoef, and Z. Su, "An integrated model of soil-canopy spectral radiances, photosynthesis, fluorescence, temperature and energy balance," *Biogeosciences,* vol. 6, no. 12, pp. 3109–3129, 2009.

[28] P. M. Anthoni *et al.*, "Forest and agricultural land-use-dependent CO_2 exchange in Thuringia, Germany," *Global Change Biol.,* vol. 10, no. 12, pp. 2005–2019, 2004.

[29] A.-K. Prescher, T. Grünwald, and C. Bernhofer, "Land use regulates carbon budgets in eastern Germany: From NEE to NBP," *Agricultural Forest Meteorol.,* vol. 150, no. 7/8, pp. 1016–1025, 2010.

[30] S. B. Verma *et al.*, "Annual carbon dioxide exchange in irrigated and rainfed maize-based agroecosystems," *Agricultural Forest Meteorol.,* vol. 131, no. 1-2, pp. 77–96, 2005.

[31] K. S. Hemes *et al.*, "Assessing the carbon and climate benefit of restoring degraded agricultural peat soils to managed wetlands," *Agricultural Forest Meteorol.,* vol. 268, pp. 202–214, 2019.

[32] X. Li, J. Xiao, J. B. Fisher, and D. D. Baldocchi, "ECOSTRESS estimates gross primary production with fine spatial resolution for different times of day from the international space station," *Remote Sens. Environ.,* vol. 258, 2021, Art. no. 112360.

[33] T. Wutzler *et al.*, "Basic and extensible post-processing of eddy covariance flux data with REddyProc," *Biogeosciences,* vol. 15, no. 16, pp. 5015–5030, 2018.

[34] M. Reichstein *et al.*, "On the separation of net ecosystem exchange into assimilation and ecosystem respiration: Review and improved algorithm," *Global Change Biol.,* vol. 11, no. 9, pp. 1424–1439, 2005.

[35] P. J. Curran, and C. M. Steele, "MERIS: The re-branding of an ocean sensor," *Int. J. Remote Sens.,* vol. 26, no. 9, pp. 1781–1798, 2005.

[36] M. Rast, J. L. Bezy, and S. Bruzzi, "The ESA medium resolution imaging spectrometer MERIS a review of the instrument and its mission," *Int. J. Remote Sens.,* vol. 20, no. 9, pp. 1681–1702, 1999.

[37] X. Qian and L. Liu, "Retrieving crop leaf chlorophyll content using an improved look-up-table approach by combining multiple canopy structures and soil backgrounds," *Remote Sens.,* vol. 12, no. 13, 2020, Art. no. 2139.

[38] A. A. Gitelson, "Wide dynamic range vegetation index for remote quantification of biophysical characteristics of vegetation," *J. Plant Physiol.,* vol. 161, no. 2, pp. 165–173, 2004.

[39] A. L. Nguy-Robertson *et al.*, "Estimating green LAI in four crops: Potential of determining optimal spectral bands for a universal algorithm," *Agricultural Forest Meteorol.,* vol. 192, pp. 140–148, 2014.

[40] Y. Peng and A. A. Gitelson, "Application of chlorophyll-related vegetation indices for remote estimation of maize productivity," *Agricultural Forest Meteorol.,* vol. 151, no. 9, pp. 1267–1276, 2011.

[41] A. D. Friend, "PGEN: An integrated model of leaf photosynthesis, transpiration, and conductance," *Ecol. Model.,* vol. 77, no. 2-3, pp. 233–255, 1995.

[42] J. Verrelst *et al.*, "Evaluating the predictive power of sun-induced chlorophyll fluorescence to estimate net photosynthesis of vegetation canopies: A SCOPE modeling study," *Remote Sens. Environ.,* vol. 176, pp. 139–151, 2016.

[43] M. Xu *et al.*, "Retrieving leaf chlorophyll content using a matrix-based vegetation index combination approach," *Remote Sens. Environ.,* vol. 224, pp. 60–73, Apr. 2019.

[44] S. Jay, F. Maupas, R. Bendoula, and N. Gorretta, "Retrieving LAI, chlorophyll and nitrogen contents in sugar beet crops from multi-angular optical remote sensing: Comparison of vegetation indices and PROSAIL inversion for field phenotyping," *Field Crops Res,* vol. 210, pp. 33–46, Aug. 2017.

[45] S. D. Wullschleger, "Biochemical limitations to carbon assimilation in C3 plants—A retrospective analysis of the A/Ci curves from 109 species," *J. Exp. Botany,* vol. 44, no. 5, pp. 907–920, 1993.

[46] J. Kattge, W. Knorr, T. Raddatz, and C. Wirth, "Quantifying photosynthetic capacity and its relationship to leaf nitrogen content for global-scale terrestrial biosphere models," *Global Change Biol.,* vol. 15, no. 4, pp. 976–991, 2009.

[47] X. Luo, H. Croft, J. M. Chen, L. He, and T. F. Keenan, "Improved estimates of global terrestrial photosynthesis using information on leaf chlorophyll content," *Global Change Biol.,* vol. 25, no. 7, pp. 2499–2514, 2019.

[48] C. Brümmer *et al.*, "How climate and vegetation type influence evapotranspiration and water use efficiency in Canadian forest, peatland and grassland ecosystems," *Agricultural Forest Meteorol.,* vol. 153, pp. 14–30, 2012.

[49] E. Falge *et al.*, "Phase and amplitude of ecosystem carbon release and uptake potentials as derived from FLUXNET measurements," *Agricultural Forest Meteorol.,* vol. 113, no. 1–4, pp. 75–95, 2002.

[50] R. Wang, J. M. Chen, X. Luo, A. Black, and A. Arain, "Seasonality of leaf area index and photosynthetic capacity for better estimation of carbon and water fluxes in evergreen conifer forests," *Agricultural Forest Meteorol.,* vol. 279, 2019, Art. no. 107708.

[51] J. Kala *et al.*, "Influence of leaf area index prescriptions on simulations of heat, moisture, and carbon fluxes," *J. Hydrometeorol.,* vol. 15, no. 1, pp. 489–503, 2014.

[52] H. Fang, F. Baret, S. Plummer, and G. Schaepman-Strub, "An overview of global leaf area index (LAI): Methods, products, validation, and applications," *Rev. Geophys.,* vol. 57, no. 3, pp. 739–799, 2019.

[53] J. Verrelst, J. P. Rivera, C. van der Tol, F. Magnani, G. Mohammed, and J. Moreno, "Global sensitivity analysis of the SCOPE model: What drives simulated canopy-leaving sun-induced fluorescence?," *Remote Sens. Environ.,* vol. 166, pp. 8–21, 2015.

Xidong Chen received the B.S. degree in remote sensing science and technology from Henan Polytechnic University, Jiaozuo, China. He is currently working toward the Ph.D. degree at the Aerospace Information Research Institute, Chinese Academy of Sciences, Beijing, China.

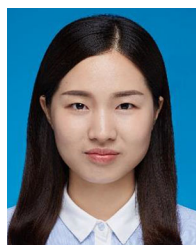His research interests include quantitative remote sensing of land surfaces and remote sensing classification

Xiaojin Qian received the B.S. degree in remote sensing science and technology from Jiangsu Normal University, Xuzhou, China. She is currently working toward the Ph.D. degree at the Aerospace Information Research Institute, Chinese Academy of Sciences, Beijing, China.

Her research interest is vegetation quantitative remote sensing.

Liangyun Liu received the B.S. degree in physics in 1996 from Huaibei Normal University, Huaibei, China and the Ph.D. degree in optics in 2000 from Xi'an Institute of Optics and Precision Mechanics, Chinese Academy of Sciences, Xi'an, China.

He is currently a Research Professor with the Aerospace Information Research Institute, Chinese Academy of Sciences, Beijing, China. He has authored or coauthored more than 200 journal papers in vegetation quantitative remote sensing.

Dr. Liu was awarded by five government's prizes, including two second-class National Scientific and Technological Progress Award, and also honored by the National Science Fund for Distinguished Young Scholars in 2018.

Pablo J. Zarco-Tejada received the degree in agricultural engineering from the University of Córdoba, Córdoba, Spain, the M.Sc. degree in remote sensing from the University of Dundee, Scotland, U.K., and the Ph.D. degree in earth and space science from York University, Toronto, ON, Canada.

He has been a Faculty Member for remote sensing at the University of California, Davis, CA, USA, the Director of the Institute for Sustainable Agriculture, National Research Council (CSIC, Spain), and a Senior Scientist with the Joint Research Centre, European Commission, Brussels, Belgium. He is currently a Professor in remote sensing and precision agriculture with the School of Agriculture and Faculty of Engineering, University of Melbourne, Parkville VIC, Australia, and an Honorary Scientist with Instituto de Agricultura Sostenible-CSIC, Córdoba, Spain. As the Leader of the HyperSens Laboratory, he focuses on remote sensing for biotic and abiotic crop and forest stress detection using hyperspectral and thermal images acquired by manned and unmanned aircraft systems. A highly cited researcher in 2019 and 2020, he is the author of more than 150 papers published in international journals.

Dr. Zarco-Tejada is currently an Associate Editor of *Remote Sensing of Environment and European Journal of Agronomy journals*, and was the recipient of awards in Spain, the United Kingdom, and Canada.